

## Gas-Liquid Interfacial Area, Bubble Size and Liquid-Phase Mass Transfer Coefficient in a Three-Phase External Loop Airlift Bubble Column

M. Yoshimoto, S. Suenaga, K. Furumoto\*, K. Fukunaga, and Katsumi Nakao<sup>†</sup>

Department of Applied Chemistry and Chemical Engineering,  
Yamaguchi University, Tokiwadai, Ube, Yamaguchi 755-8611, Japan  
e-mail: knakao@yamaguchi-u.ac.jp

\*Oshima National College of Maritime Technology, Oshima,  
Yamaguchi 742-2106, Japan

Original scientific paper  
Received: May 29, 2007  
Accepted: October 15, 2007

The interfacial area  $a$  was measured by the sulfite oxidation method in a three-phase external loop airlift bubble column suspending completely the different concentrations of ion exchange resin particles in aqueous carboxymethyl cellulose (CMC) solutions with a wide range of viscosity. The column had been previously studied for the circulating liquid velocity  $U_L$ , gas holdup  $\varepsilon_G$  and volumetric gas-liquid oxygen transfer coefficient  $k_L a$  in the two- and three-phase systems. The average bubble size  $d_B$  and oxygen transfer coefficient  $k_L$  were obtained as  $d_B = 6 \varepsilon_G / a$  and  $k_L = (\text{the previous } k_L a) / a$ , respectively. The similar studies were carried out in the internal loop airlift and normal bubble columns for comparison. The  $a$  values in the external loop airlift were found to be little affected by the column height and particles concentrations, and to decrease with increasing viscosity. All the three columns showed a linear dependence of  $a$  on  $\varepsilon_G$ . A simple correlation of  $a$ ,  $d_B$  or  $k_L$  was proposed as a function of  $\varepsilon_G$  and viscosity for the external loop airlift as well as both internal loop airlift and normal columns. A well-known relationship between  $k_L$  and  $d_B$  was confirmed to hold independent of column types and operating conditions for a given two or three phase system.

*Key words:*

External loop airlift, three phase flow, suspended solid particles, interfacial area, bubble size, oxygen transfer coefficient

### Introduction

Much work has been done on the hydrodynamics and mass transfer in the gas-liquid two phase flow in the external loop airlift bubble column (ELBC).<sup>1-4</sup> The unique feature of ELBC is its more well-defined recirculating liquid flow pattern which makes the hydrodynamic and mass transfer properties different from those in the internal loop airlift bubble column (ILBC) and normal bubble column (NBC). Especially, the liquid circulation makes it easier for the solid particles charged to be completely and uniformly suspended in ELBC than in either ILBC or NBC. Recently, more attention has been paid to the hydrodynamics and mass transfer in the gas-liquid-solid three phase flow in ELBC.<sup>5-7</sup> The effects of suspended solid particles on the gas holdup  $\varepsilon_G$  and volumetric gas-liquid mass transfer coefficient  $k_L a$  have extensively been studied in the three phase ELBC.<sup>8,9</sup> Although there have been a few studies on the gas-liquid interfacial area  $a$  in the two phase ELBC,<sup>3,4</sup> however, little work has been carried out on  $a$  in the three phase ELBC. The data on  $a$  provide the results on the average bubble

diameter  $d_B$  and gas-liquid mass transfer coefficient  $k_L$  calculated as  $d_B = 6\varepsilon_G/a$  and  $k_L = k_L a/a$ , respectively. These informations suggest the behavior of bubbles such as the bubble coalescence and breakup which are governed by the system and operating variables as well as the bubble column designs, and are used to determine the column characteristics including  $\varepsilon_G$ ,  $k_L a$ ,  $a$  etc.

The purpose of this work is to (a) measure  $a$  by the sulfite oxidation method in the two- and three-phase flows in ELBC as well as both ILBC and NBC, (b) determine  $d_B$  from the  $a$  and  $\varepsilon_G$  values observed simultaneously and  $k_L$  from dividing by  $a$  the  $k_L a$  values observed in tap water with and without carboxymethyl cellulose (CMC) separately, (c) examine the effects on the  $a$ ,  $d_B$  and  $k_L$  values of the suspended solid particles, liquid viscosity, superficial gas velocity and bubble column design, and (d) correlate the data on  $a$ ,  $d_B$  and  $k_L$  with  $\varepsilon_G$  and the peculiar liquid viscosity  $\mu_p$  easily measured by the Ostwald-type viscometer based on our previous correlations of  $\varepsilon_G$  and  $k_L a$  for the two phase flow.<sup>2</sup>

<sup>†</sup>Corresponding author

## Experimental

The apparatus used were almost the same as those in our previous work on the gas-liquid two phase flows.<sup>2</sup> Fig. 1(a) shows a schematic diagram of the external loop airlift bubble column (ELBC). As shown in Fig. 1(b), the internal loop airlift bubble column (ILBC) had a draft tube of 5 cm in diameter with gas injection into the annular section of the ILBC. The 9.5 mm porcelain Raschig rings were packed beneath the perforated plate. The ILBC was used as the normal bubble column (NBC) by removing the draft tube. Table 1 summarizes the experimental conditions.

The values of  $k_L a$  were previously obtained by carrying out both the desorption of dissolved oxygen into nitrogen gas flow and the absorption of oxygen in air flow into the aqueous phase in the three phase column.<sup>10</sup> The time course of the dissolved oxygen electrode inserted in the liquid phase through the column wall as shown in Fig. 1(a). The liquids used were tap water and aqueous 0.5 to 2.0 % carboxymethyl cellulose (CMC) solutions. CMC was used to increase the liquid viscosity.

The gas holdup  $\varepsilon_G$  in the gas-liquid-solid three phase flow in the riser of the ELBC was determined from an analysis of the gradient of static pressure along the column height considering the pressure due to suspended solid particles. The  $\varepsilon_G$  values in the ILBC and NBC were measured by the volume expansion method.

The circulating superficial liquid velocity  $U_L$  in the three phase flow through the riser was measured in the same way as in the two phase flow in our previous work<sup>2,10</sup> using a plastic sphere of 1.2 cm diameter having the same density as the liquid

Table 1 – Experimental conditions for specific interfacial area

Gas: Air, Superficial gas velocity $U_G = 0.02 \sim 0.32$ m/s
Liquid: Aqueous sodium sulphite solution
0.5 kmol/m <sup>3</sup> Na <sub>2</sub> SO <sub>3</sub> /, 0.8, 1.2 wt% CMC/Tap water
Cobalt catalyst conc. $C_{CoSO_4} = 5 \times 10^{-4}$ kmol/m <sup>3</sup> , pH = 8.5
Static liquid height $H_T = 1 \sim 4$ m (ELBC), 0.8 m (ILBC, NBC)
Solid: Ion exchange resin (IR) ( $d_p = 450 \mu\text{m}$ , $\rho_s = 1252$ kg/m <sup>3</sup> )
Solid concentration $C_s = 0 \sim 0.10$ kg/dm <sup>3</sup> -slurry
Temp.: 298~300K

phase in the downcomer almost free of gas bubbles. The velocity in the downcomer was multiplied by the ratio of downcomer cross sectional area  $A_d$  to riser one  $A_r$  to obtain the  $U_L$  value.

The rheological properties of the CMC solutions without salts for the previous determination of  $k_L a$  were measured at 298 K with a concentric cylinder viscometer. The values of both the fluid consistency index  $K$  and the flow behavior index  $n$  were reported in our previous paper.<sup>2</sup> For convenience, the peculiar viscosity  $\mu_p$  was also measured using a Ostwald-type viscometer. The  $a$  value were measured at room temperature (293 to 300 K) in the case of water without CMC. The temperature of the solution with CMC in the taller ELBC was kept at almost constant of 298 K by a temperature controller unit installed in the gas-liquid separator since a higher liquid viscosity was more sensitive to a change in temperature.

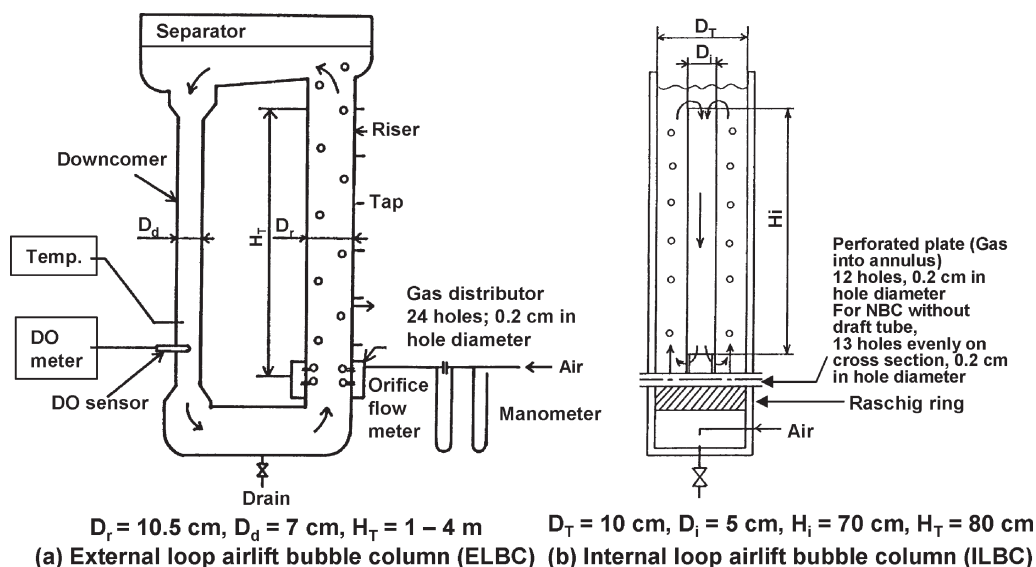


Fig. 1 – Experimental apparatus. (a) External loop airlift bubble column (ELBC), (b) Internal loop airlift bubble column (ILBC)

The liquid used for measurement of  $a$  was tap water containing  $0.5 \text{ kmol/m}^3$  sodium sulfite  $\text{Na}_2\text{SO}_3$  and  $5 \cdot 10^{-4} \text{ kmol/m}^3$  cobalt sulfate  $\text{CoSO}_4$  as a catalyst for the sulfite oxidation by air. The chemical oxygen absorption rate  $R_{\text{O}_2}$  [ $\text{kmol/m}^3\text{s}$ ] based on the liquid volume was obtained as one half of the rate of decrease in the sulfite concentration which was determined by iodometric titration. CMC was added to the sulfite solution to vary the liquid viscosity. The viscosity was measured by the same Ostwalde-type viscometer as described above. The ion exchange resin (IR) particles of  $450 \mu\text{m}$  in mean diameter were used to examine an effect of suspended solid particles on  $a$ .

### Measurement of gas-liquid interfacial area $a$

According to the previous kinetic studies on the oxidation of  $\text{Na}_2\text{SO}_3$  by air based on the chemical absorption theory,<sup>11</sup> the absorption rate  $R_{\text{O}_2}$  is expressed by the following equation, which holds for the pseudo first order regime in the theory.

$$R_{\text{O}_2} = \{a/(1-\varepsilon_G-\varepsilon_S)\} \{(2/3)k_2D_{\text{O}_2}\}^{1/2}C_{\text{O}_i}^{3/2} \quad (1)$$

Where  $a$  is the interfacial area based on the dispersion volume,  $\varepsilon_S = (1-\varepsilon_G)C_S/\rho_S$  the solid holdup,  $k_2$  [ $\text{m}^3/\text{kmol} \cdot \text{s}$ ] the rate constant for the reaction of the second and zero-th order with respect to the dissolved oxygen and sulfite concentration, respectively,  $D_{\text{O}_2}$  [ $\text{m}^2/\text{s}$ ] the liquid diffusivity of oxygen and  $C_{\text{O}_i}$  [ $\text{kmol/m}^3$ ] the dissolved oxygen concentration at the gas-liquid interface calculated from the oxygen partial pressure in the gas phase  $P_{\text{O}_2}$  [Pa] and Henry's law constant  $H$  [ $\text{kmol/Pa} \cdot \text{m}^3$ ] as  $C_{\text{O}_i} = H P_{\text{O}_2}$ .

From the analysis on the kinetic data on the sulfite oxidation by air carried out in the stirred cell with a known flat gas-liquid interface, i.e., a known value of  $a$  in Eq. (1),  $k_2$  was determined under the condition of  $C_{\text{Na}_2\text{SO}_3} = 0.5 \text{ kmol/m}^3$ ,  $\text{pH} = 8.5$  and  $T = 288\text{--}308 \text{ K}$  as follows.

$$k_2 = 2.36 \times 10^{19} C_{\text{CaSO}_4} \exp(-5.13 \times 10^7/RT) \quad (2)$$

where  $R = 8.314 \text{ Pa} \cdot \text{m}^3/\text{kmol} \cdot \text{K}$  is the gas constant and  $C_{\text{CoSO}_4}$  [ $\text{kmol/m}^3$ ] is the  $\text{CoSO}_4$  catalyst concentration. Addition of CMC to the solution exerted no effect on the  $k_2$  value. The chemical absorption theory with the result of Eq. (2) verifies that the above conditions of  $0.5 \text{ kmol/m}^3 \text{ Na}_2\text{SO}_3$ ,  $5 \times 10^{-4} \text{ kmol/m}^3 \text{ CoSO}_4$ ,  $\text{pH} = 8.5$  and  $T = 293\text{--}300 \text{ K}$  satisfy the requirements for the pseudo first order regime, i.e., Eq. (1). Therefore, the  $a$  values in any type of bubble columns can be obtained from the following Eq. (1a) by measuring the  $R_{\text{O}_2}$  values.

$$a = R_{\text{O}_2}(1 - \varepsilon_G - \varepsilon_S)/[\{(2/3)k_2D_{\text{O}_2}\}^{1/2}C_{\text{O}_i}^{3/2}] \quad (1a)$$

In the case of ELBC, the  $R_{\text{O}_2}$  value above should be obtained by noting that the observed sulfite concentrations were always diluted due to the downcomer under the assumption of the well mixed flow in the whole column. Thus, the apparent value of  $R_{\text{O}_2}$ ,  $R_{\text{O}_2}^{\text{app}}$ , was converted to the  $R_{\text{O}_2}$  value in the riser in the following way.

$$R_{\text{O}_2} = R_{\text{O}_2}^{\text{app}}(V_L/V_{\text{Lr}}) \quad (3)$$

where  $V_L$  and  $V_{\text{Lr}}$  are the total and riser liquid volumes, respectively. Assuming the gas phase in plug flow in any type of columns, the  $C_{\text{O}_i}$  value in Eq. (1a) was determined as the value in equilibrium with the average oxygen partial pressure  $\bar{P}_{\text{O}_2}$ , i.e.,  $C_{\text{O}_i} = H\bar{P}_{\text{O}_2}$ . The  $\bar{P}_{\text{O}_2}$  value was calculated as the logarithmic mean of the inlet and outlet oxygen partial pressures. The latter pressure was determined from the oxygen balance with the  $R_{\text{O}_2}$  value above.

The average bubble diameter  $d_B$  was calculated from the observed values of  $\varepsilon_G$  and  $a$  as follows.

$$d_B = 6\varepsilon_G/a \quad (4)$$

The liquid phase oxygen transfer coefficient  $k_L$  was calculated from dividing by the observed  $a$  value the corresponding  $k_L a$  value for the two phase having the same liquid viscosity as the three phase concerned.

$$k_L = k_L a/a \quad (5)$$

The determination was based on the facts that the  $k_L a$  values in the three phase ELBC were reproduced by the  $k_L a$  correlation for the two phase ELBC<sup>10</sup> and that even in the case of NBC, of which characteristics are known to be more sensitive to the liquid properties compared to ELBC, the  $k_L a$  values determined in the CMC solution containing sodium sulfate followed their  $k_L a$  correlation proposed for pure CMC solution.<sup>12</sup> Analogously, the  $d_B$  and  $k_L$  values for both ILBC and NBC were calcu-

Table 2 - Correlations for  $U_L$ ,  $\varepsilon_G$  and  $k_L a$  in gas-liquid system using  $\mu_P^2$

ELBC	$U_L = 1.80 (A_d/A_r)^{0.75} U_G^{0.40} \mu_P^{-0.028} H_T^{0.31}$	$(\mu_P \leq 0.04 \text{ Pa} \cdot \text{s})$ (6a)
	$U_L = 0.67 (A_d/A_r)^{0.75} U_G^{0.40} \mu_P^{-0.33} H_T^{0.31}$	$(\mu_P > 0.04 \text{ Pa} \cdot \text{s})$ (6b)
ELBC	$U_G/\varepsilon_G = \{0.49 + 2.25 (U_G + U_L)\} \mu_P^{0.103}$	(7)
ILBC, NBC	$U_G/\varepsilon_G = 0.49 \mu_P^{0.103} + 2.4 U_G$	(8)
ELBC	$k_L a = 6.60 \times 10^{-2} \varepsilon_G^{1.2} \mu_P^{-0.36}$	(9)
ILBC, NBC	$k_L a = 3.35 \times 10^{-2} \varepsilon_G^{1.1} \mu_P^{-0.33}$	(10)

lated. Table 2 shows our previous correlations of  $k_L a$  for the two phase flow ELBC, ILBC and NBC using the peculiar liquid viscosity  $\mu_p$  for convenience.<sup>2</sup> The table also includes the correlations of  $U_L$  in ELBC and the correlations of  $\varepsilon_G$  in three types of columns.

### Results and discussion

#### Effect of static liquid height $H_T$ on interfacial area $a$ and gas holdup $\varepsilon_G$ in ELBC

Fig. 2(a) and 2(b) show respectively the  $a$  and  $\varepsilon_G$  values in ELBC using aqueous 0.5 kmol/m<sup>3</sup> Na<sub>2</sub>SO<sub>3</sub> solution as a function of the superficial gas velocity  $U_G$  with  $H_T$  as a parameter. The  $a$  values are seen to be almost unaffected by  $H_T$  and to show almost the same variation with  $U_G$  in the range of  $U_G$  less than 0.1 m/s as those reported by Popovic & Robinson (1987a)<sup>3</sup>, while the  $\varepsilon_G$  values to be a little affected by  $H_T$  as represented by the previous correlation Eq. (7) shown in Table 2. The former result may be due the fact that the bubble coalescence was retarded by the higher upward liquid velocity with the higher  $H_T$  as well as the presence of a coalescence-inhibiting electrolyte Na<sub>2</sub>SO<sub>3</sub>. The variation of  $a$  with  $U_G$  are found to be parallel to that of  $\varepsilon_G$ . The circulating liquid superficial velocity  $U_L$  in

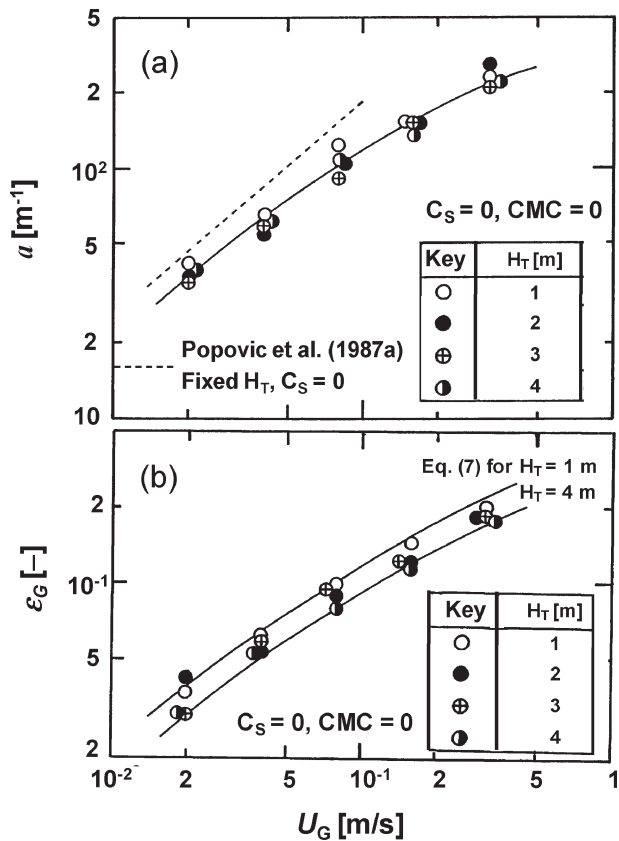


Fig. 2 - Effect of  $H_T$  on (a)  $a$  and (b)  $\varepsilon_G$  as a function of  $U_G$  (ELBC)

the riser was also observed to agree well with the previous  $U_L$  correlation Eq. (6a).

#### Effect of liquid viscosity on $a$ and $\varepsilon_G$

Fig. 3(a) and 3(b) show the variations of the  $a$  and  $\varepsilon_G$  values with  $U_G$ , respectively, in three types of bubble columns with the liquid viscosity as a parameter. It is seen in the figures that the variation of  $a$  with  $U_G$  is parallel to that of  $\varepsilon_G$  at any viscosity in any type of columns, that  $a$  decreases with increasing viscosity in any column while  $\varepsilon_G$  is little affected by the viscosity, and that the  $a$  values in three columns have almost the same value at a fixed liquid viscosity although the  $\varepsilon_G$  values in the ILBC and NBC are larger than the those in the ELBC. These results on  $a$  arise from an enhancement of bubble coalescence due to increased viscosity in any column and a more retardation of bubble coalescence in the ELBC than in ILBC and NBC due to a higher upward liquid velocity in the riser. On

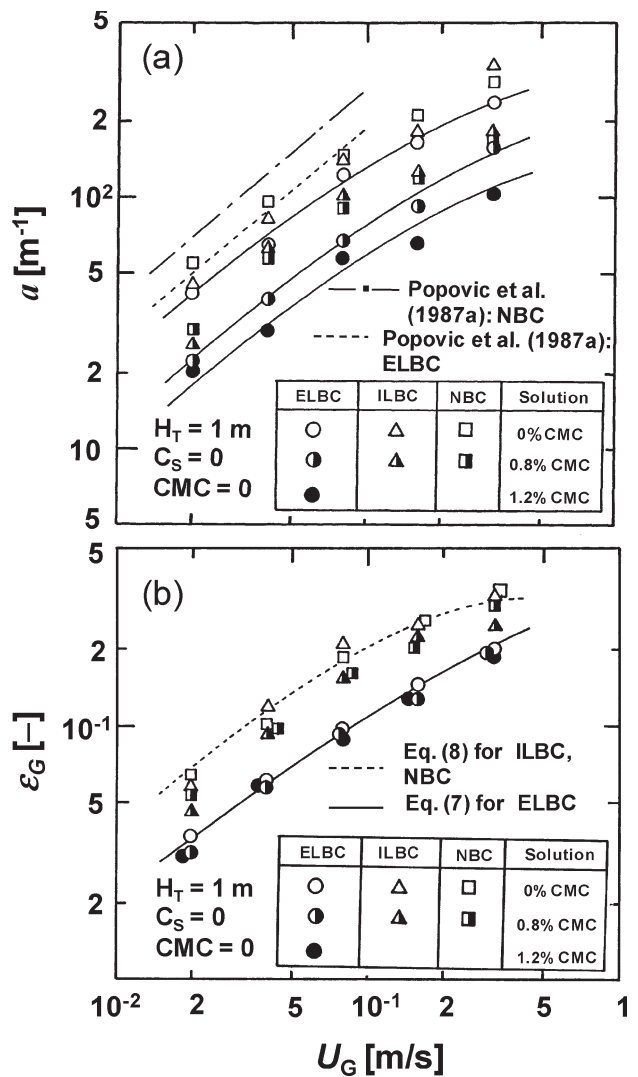


Fig. 3 - Effect of liquid viscosity on (a)  $a$  and (b)  $\varepsilon_G$  as a function of  $U_G$

the other hand, the liquid velocity causes the lower  $\epsilon_G$  value in the ELBC compared to that in either ILBC or NBC. The  $\epsilon_G$  values observed in the ELBC as well as the ILBC and NBC are found to agree with those calculated respectively by Eq. (7) and Eq. (8) in Table 2.

**Effect of solid particles concentration  $C_S$  on  $a$  and  $\epsilon_G$**

Fig. 4(a) and 4(b) represent the change of the  $a$  and  $\epsilon_G$  values with  $U_G$ , respectively, in the three bubble columns with  $C_S$  as a parameter. Fig. 4(a) suggests that the suspended solid particles increase the  $a$  value a little under a certain condition. This may be due to an enhancement of bubble breakup by suspended solid particles. Because of no clear tendency and a small effect exerted by the particles, the effect of particles on  $a$  is considered to be neglected in the sulfite solution. No effect of particles on  $\epsilon_G$  in any column is more clearly shown in Fig. 4(b). The  $\epsilon_G$  values are also seen to be reproduced by Eqs. (7) and (8) in Table 2.

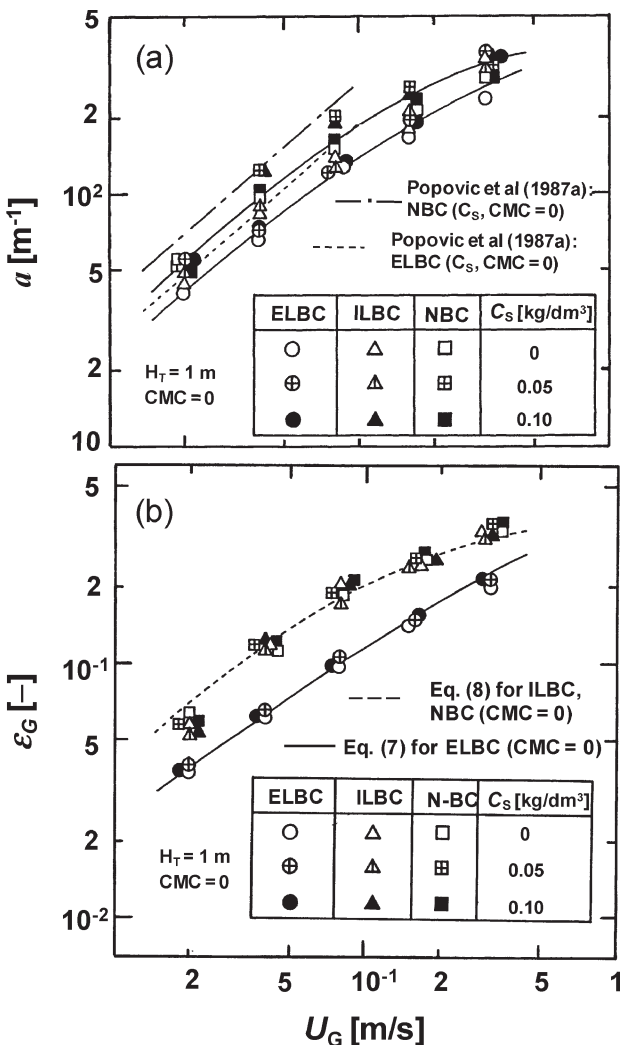


Fig. 4 – Effect of  $C_S$  on (a)  $a$  and (b)  $\epsilon_G$  as a function of  $U_G$

**Dependence of  $d_B$  on  $H_T$ , liquid viscosity and  $C_S$**

Fig. 5(a), 5(b) and 5(c) show the  $d_B$  values calculated by Eq. (4) as a function of  $U_G$  with the parameters of the  $H_T$  in ELBC and the liquid viscosity and  $C_S$  in three columns, respectively. It is seen in the figures that the  $d_B$  values are approximately independent of  $U_G$  in any values of  $H_T$ , liquid viscosity and  $C_S$ , that at a fixed value of  $U_G$ ,  $H_T$  exerts no effect on  $d_B$  in ELBC, that in any type of column,  $C_S$  slightly influences  $d_B$  although no clear tendency is found and hence is regarded to unaffected  $d_B$ , and that increasing the liquid viscosity clearly increases  $d_B$ .

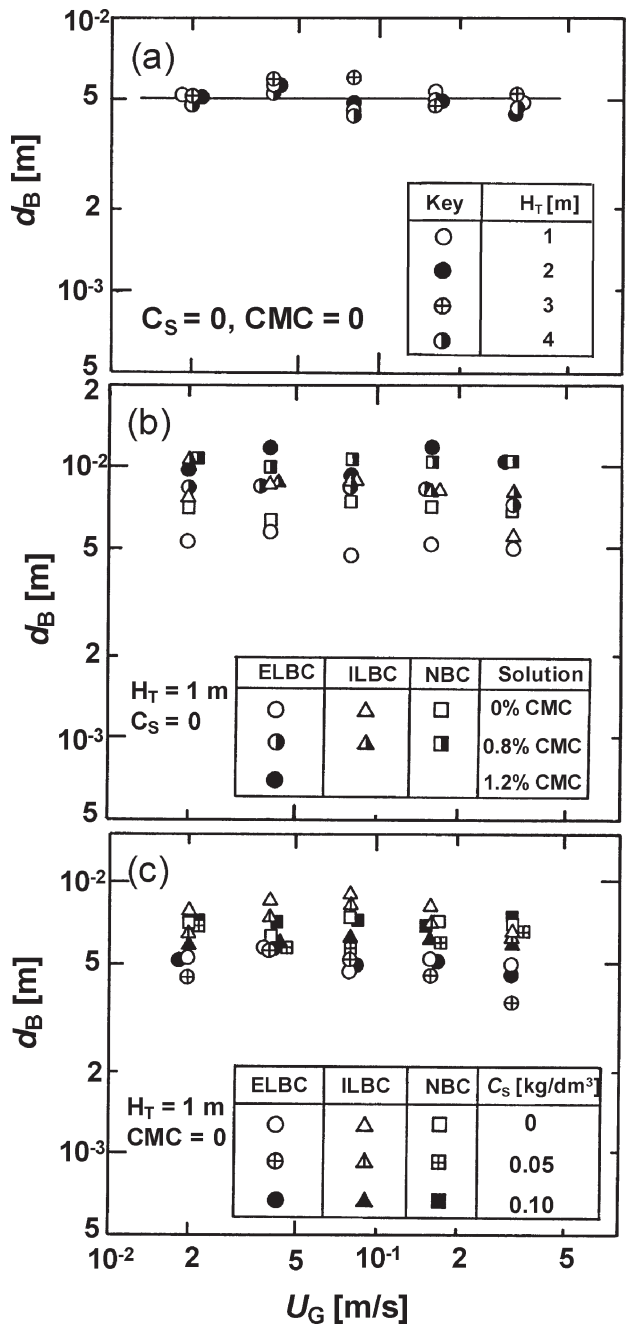


Fig. 5 – Effects of (a)  $H_T$ , (b) liquid viscosity and (c)  $C_S$  on  $d_B$  as a function of  $U_G$

due to an enhanced bubble coalescence in the more viscous solution. A complicated small variation of  $d_B$  with  $U_G$  at any values of  $H_T$ , liquid viscosity and  $C_S$  suggests an interaction among these variables governing a balance between the bubble coalescence and breakup frequencies. It is also noted that the  $d_B$  value in the ELBC is lower than that in either ILBC or NBC under the same conditions of  $U_G$ , viscosity and  $C_S$  because of a retarded bubble coalescence caused by a high upward liquid velocity in the riser of ELBC. The  $d_B$  values in the ILBC are found to be approximated by those in the NBC.

**Dependence of  $k_L$  on  $H_T$ , liquid viscosity and  $C_S$**

Fig. 6(a), 6(b) and 6(c) represent the variations of  $k_L$  calculated by Eq. (5) with  $U_G$  using the  $H_T$  in ELBC and the liquid viscosity and  $C_S$  in three columns as parameters, respectively. It is found in the figures that the  $k_L$  values in any systems and columns slightly increase with increasing  $U_G$  or are almost constant independent of  $U_G$  considering a small but complicated fluctuation of  $k_L$  with a wide range of change in  $U_G$ . It is also seen that  $k_L$  decreases with increasing liquid viscosity at a fixed value of  $U_G$  in any column and is little affected not only by the type of column and the  $H_T$  in the ELBC at a fixed liquid viscosity, but also by  $C_S$  except the case of  $C_S = 0.05 \text{ kg/dm}^3$  in the NBC probably having a more complicated three phase flow. Furthermore, the  $k_L$  values observed in  $0.5 \text{ kmol/m}^3 \text{ Na}_2\text{SO}_3$  solution without either CMC or  $C_S$  are shown to agree well with the literature values<sup>3</sup> in the ELBC and NBC although a small difference in the  $U_G$  dependency of  $k_L$  between them. Based on a model of mass transfer into the surface of a turbulent liquid,<sup>13,14</sup> the  $k_L$  value is shown to increase with  $U_G^{1/4}$ . Therefore, it is reasonable to conclude that the observed  $k_L$  values slightly increase with increasing  $U_G$ .

**Dependence of  $k_L$  on  $d_B$**

Fig. 7 shows a plot of the obtained  $k_L$  values as a function of the obtained  $d_B$  values for the three types of bubble columns. It is seen in the figure that there are no clear dependence of  $k_L$  on  $d_B$  in any column although the  $k_L$  value clearly decreases with increasing liquid viscosity and almost independent of the type of column,  $H_T$  in the ELBC and  $C_S$  at a fixed value of  $d_B$ . The  $k_L$  values in the solution without either CMC or  $C_S$  are also found to be almost the same as those calculated from the correlations proposed by Calderbank and Moo-Yang (1961)<sup>15</sup> and Akita and Yoshida (1974).<sup>16</sup> and the data reported by Talvy et al.<sup>14</sup> This suggests that the  $k_L$  determination employed are reasonable and useful.

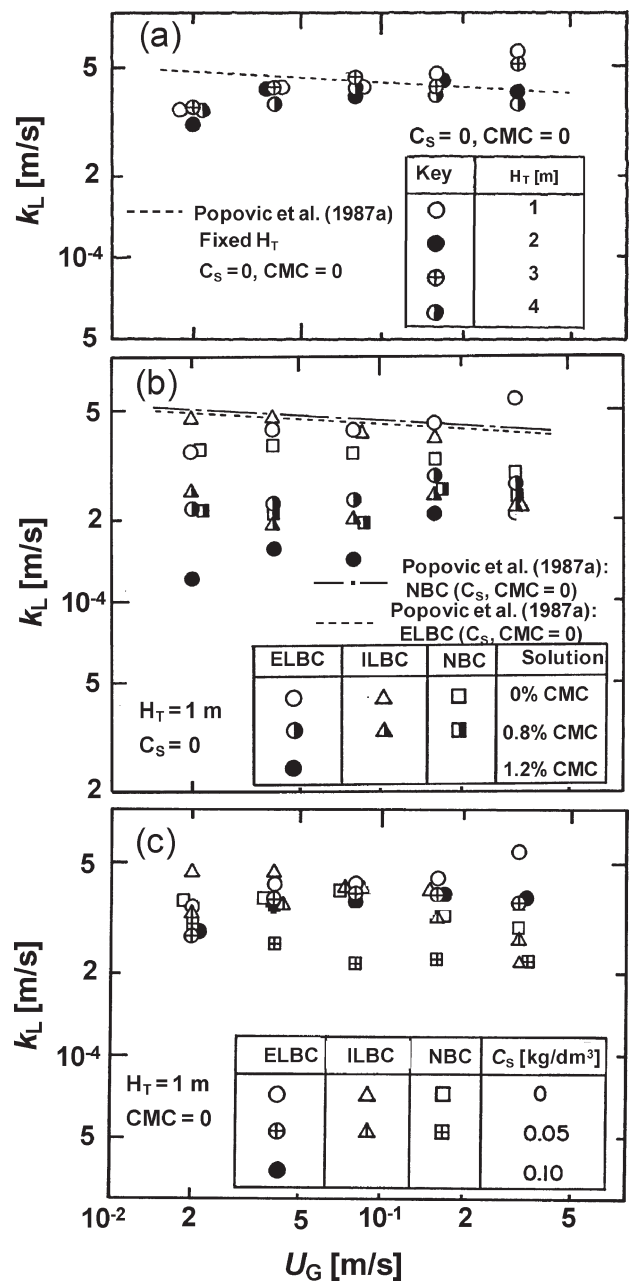


Fig. 6 – Effects of (a)  $H_T$ , (b) liquid viscosity and (c)  $C_S$  on  $k_L$  as a function of  $U_G$

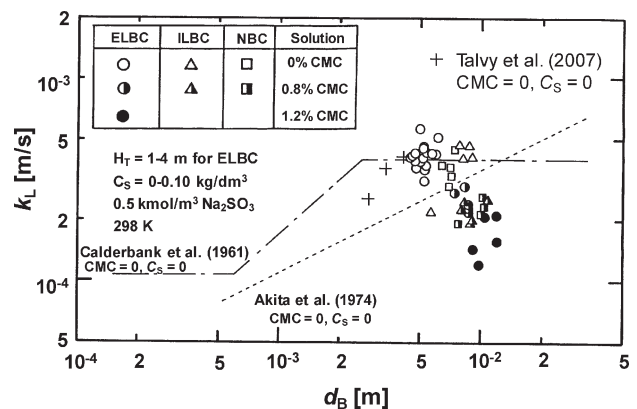


Fig. 7 – Dependence of  $k_L$  on  $d_B$

**Correlation of  $a$  with  $\epsilon_G$**

The parallel relationships between  $a$  and  $\epsilon_G$  as shown in Figs. 2, 3 and 4 lead to the plot of  $a$  as a function of  $\epsilon_G$ . Fig. 8 shows such a plot for the data obtained in the three columns with aqueous sulfite solutions containing CMC at different concentrations. All the plots of  $a$  versus  $\epsilon_G$  are seen to have the same slope of unity. Thus the values of  $a/\epsilon_G$  obtained from Fig. 8 are plotted against the peculiar viscosity  $\mu_p$  as shown in Fig. 9. Based on the figure, the correlation equations for  $a$  were obtained as Eq. (11) for ELBC and Eq. (12) for ILBC and NBC as shown in Table 3. Fig. 10 shows a comparison of the  $a$  values observed in this work with those calculated from the correlations Eqs. (11) and (12) and the literature correlation.<sup>3</sup> The present correlations Eqs (11) and (12) are found to reproduce the observed  $a$  values within an accuracy of  $\pm 20\%$ . The literature correlation well agrees with the observed  $a$  values in the range of  $U_G$  lower than 0.1 m/s and overestimate the values increasingly with increase in  $U_G$  higher than 0.1 m/s. This is partly because their ELBC column design made a part of the bubbles recirculate through the downcomer into the riser giving the larger  $\epsilon_G$  value in the whole column compared to the case of our ELBC.

The correlations of  $d_B$  for three columns were obtained by applying the correlations Eqs. (11) and (12) to Eq. (4). The results are shown in Table 3, being Eq. (13) for ELBC and Eq. (14) for ILBC and NBC. The correlations of  $k_L$  for any types of columns were derived by combining Eq. (9) with Eq. (11) for ELBC and Eq. (10) with Eq. (12) for ILBC and NBC through Eq. (5). The results are Eq. (15) for ELBC and Eq. (16) for ILBC and NBC as shown in Table 3. These correlations are very simple and useful to apply for estimating the values of  $a$ ,  $k_L$  and hence  $k_L a$  as well as  $d_B$  by knowing only both the  $\epsilon_G$  value, predicted from Eqs. (6) and (7) for ELBC and Eq. (8) for ILBC and NBC, and the  $\mu_p$  value measured simply by a Ostwalde-type viscometer. The viscometer should be calibrated with a Newtonian liquid of a known viscosity even in the case of a highly viscous liquid.

**Conclusion**

The results obtained in this work are summarized as follows.

(1) The  $a$  values in ELBC were only a little lower than those in ILBC and NBC in spite of the

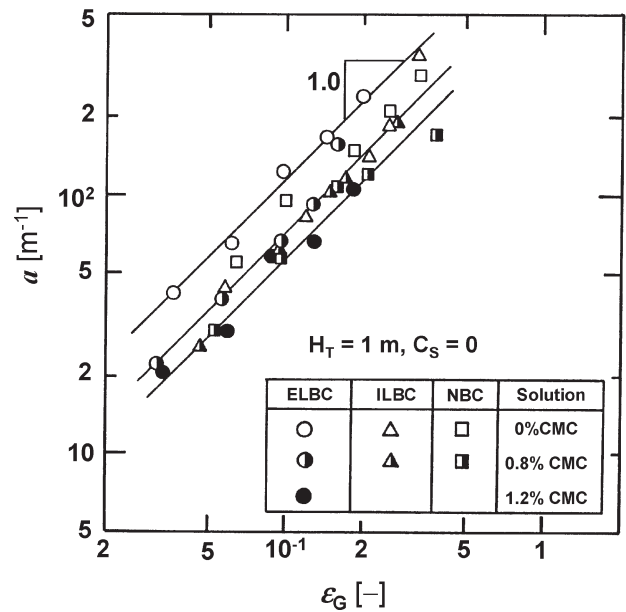


Fig. 8 – Correlation of  $a$  with  $\epsilon_G$

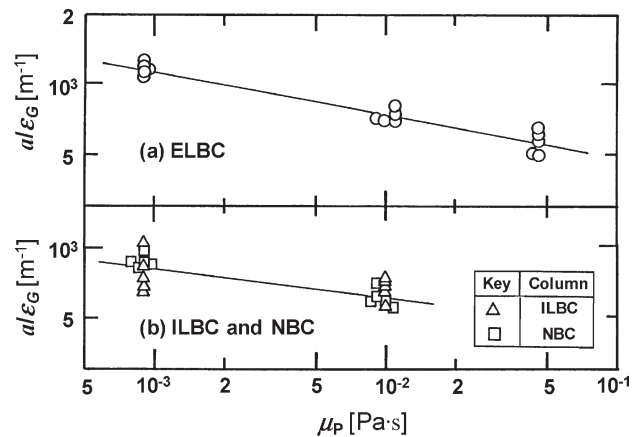


Fig. 9 – Dependence of  $a/\epsilon_G$  on  $\mu_p$

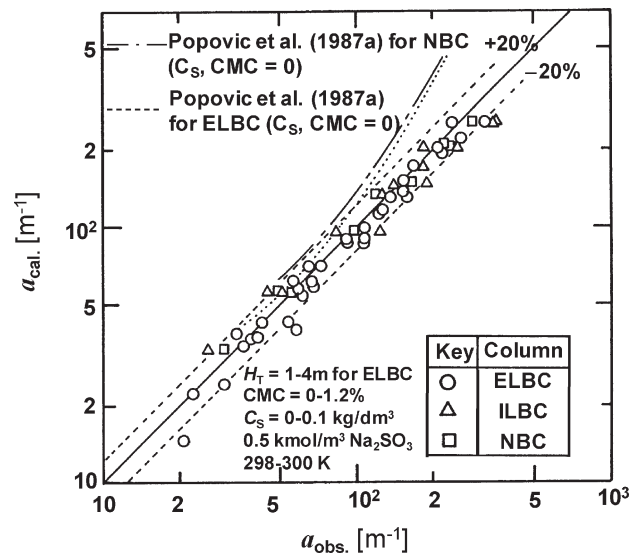


Fig. 10 – Comparison of observed  $a$  values with calculated ones from present and literature correlations

Table 3 – Correlations for  $a$ ,  $d_B$  and  $k_L$  using  $\mu_p$

ELBC: $a = 320 \epsilon_G \mu_p^{-0.18}$ (11)	ILBC, $a = 323 \epsilon_G \mu_p^{-0.13}$ (12)
$d_B = 1.88 \times 10^{-2} \mu_p^{0.18}$ (13)	NBC: $d_B = 1.86 \times 10^{-2} \mu_p^{0.13}$ (14)
$k_L = 2.07 \times 10^{-4} \epsilon_G^{0.2} \mu_p^{-0.18}$ (15)	$k_L = 1.04 \times 10^{-4} \epsilon_G^{0.1} \mu_p^{-0.20}$ (16)

lower  $\varepsilon_G$  values in ELBC compared to those in ILBC and NBC. The  $a$  values in ILBC were almost equal to those in NBC.

(2) The  $a$  values in ELBC were independent of  $H_T$  in spite of the lower  $\varepsilon_G$  for the higher  $H_T$ . This is favorable for scale-up of ELBC. The  $a$  values in any type of columns decreased with increasing liquid viscosity and the  $d_B$  values correspondingly increased keeping the  $\varepsilon_G$  values little unaffected by the viscosity. The  $a$  values in any type of columns were also unaffected by  $C_S$  since the  $\varepsilon_G$  and  $d_B$  values were little influenced by it.

(3) The  $k_L$  values in three types of columns decreased with increasing liquid viscosity and were almost independent of  $C_S$ . The  $d_B$  and  $k_L$  values in any types of columns were almost independent of  $U_G$  and those in ELBC also of  $H_T$ . The data on  $k_L$  and  $d_B$  obtained in three types of columns satisfied a well-known relationship between  $k_L$  and  $d_B$ .

(4) The simple correlation equations for  $a$ ,  $d_B$  and  $k_L$  for three types of columns were obtained as a function of  $\varepsilon_G$  and  $\mu_P$  using the previous correlations for  $\varepsilon_G$  and  $k_L a$  which were applicable to both two and three phase flows in the corresponding type of columns.

## Nomenclature

- $A_d$  – cross sectional area of downcomer,  $m^2$   
 $A_r$  – cross sectional area of riser,  $m^2$   
 $a$  – gas-liquid interfacial area,  $1/m$   
 $C_{oi}$  – dissolved oxygen concentration at gas-liquid interface,  $kmol/m^3$   
 $C_{CaSO_4}$  – cobalt sulfate (catalyst) concentration,  $kmol/m^3$   
 $C_S$  – solid particle concentration based on bubble free volume,  $kg/m^3$   
 $D_d$  – diameter of downcomer,  $m$   
 $D_i$  – diameter of draft tube,  $m$   
 $D_{O_2}$  – liquid diffusivity of oxygen,  $m^2/s$   
 $D_r$  – diameter of riser,  $m$   
 $D_T$  – diameter of ILBC and NBC,  $m$   
 $d_B$  – average bubble diameter,  $m$   
 $d_p$  – mean diameter of solid particles,  $m$   
 $H$  – Henry's law constant,  $kmol/Pa \cdot m^3$   
 $H_T$  – static liquid height above gas distributor,  $m$   
 $H_i$  – height of draft tube,  $m$   
 $K$  – fluid consistency index,  $Pa \cdot s^n$   
 $k_2$  – second order rate constant,  $m^3/kmol \cdot s$   
 $k_L$  – liquid phase oxygen transfer coefficient,  $m/s$   
 $k_L a$  – volumetric gas-liquid oxygen transfer coefficient based on dispersion volume,  $1/s$   
 $n$  – flow behavior index  
 $P_{O_2}$  – oxygen partial pressure,  $Pa$   
 $\bar{P}_{O_2}$  – average oxygen partial pressure,  $Pa$   
 $R$  – gas constant ( $= 8.314$ ),  $Pa \cdot m^3/kmol \cdot K$   
 $R_{O_2}$  – chemical oxygen absorption rate based on gas-sparged liquid volume,  $kmol/m^3 \cdot s$   
 $R_{O_2}^{app}$  – chemical oxygen absorption rate based on total liquid volume in ELBC,  $kmol/m^3 \cdot s$

- $T$  – temperature,  $K$   
 $U_G$  – superficial gas velocity,  $m/s$   
 $U_L$  – superficial liquid velocity in riser,  $m/s$   
 $V_L$  – total liquid volume in ELBC,  $m^3$   
 $V_{L,r}$  – riser liquid volume,  $m^3$

## Greek letters

- $\varepsilon_G$  – gas holdup  
 $\varepsilon_S$  – solid holdup ( $= (1 - \varepsilon_G) C_S/\rho_S$ )  
 $\mu_P$  – peculiar viscosity measured by Ostwalde-type viscometer,  $Pa \cdot s$   
 $\rho_S$  – density of solid particle,  $kg/m^3$

## Subscripts

- cal – calculated value  
 obs – observed value

## List of abbreviations

- CMC – carboxymethyl cellulose  
 ELBC – external loop airlift bubble column  
 ILBC – internal loop airlift bubble column  
 IR – ion exchange resin  
 NBC – normal bubble column

## References

- Chisti, M. Y., "Airlift bioreactors" Elsevier Applied Science, New York, NY (1989)
- Nakao, K., Suenaga, S., Takeda, K., Kimura, M., Robinson, C. W., "Mass Transfer in a Bubble Column with External Liquid Circulation" Preprints of 1st German-Japanese Symp. Bubble Columns, Schwerte, Germany, June 13-15, 1988, p.153-158.
- Popovic, M., Robinson, C. W., Chem. Eng. Sci. **42** (1987a) 2811.
- Popovic, M., Robinson, C. W., Chem. Eng. Sci. **42** (1987b) 2825.
- Douek, R. S., Livingston, A. G., Johansson, A. C., Hewitt, G. F., Chem. Eng. Sci. **49** (1994) 3719.
- Merchuk, J. C., Can. J. Chem. Eng. **81** (2003) 324.
- Nakao, K., Azakami, F., Furumoto, K., Yoshimoto, M., Fukunaga, K., Can. J. Chem. Eng. **81** (2003) 444.
- Freitas, C., Fialova, M., Zahradnik, J., Teixeira, J. A., Chem. Eng. Sci. **54** (1999) 5253.
- Nakao, K., Harada, T., Furumoto, K., Kiefner, A., Popovic, M., Can. J. Chem. Eng. **77** (1999) 816.
- Nakao, K., Suenaga, S., Furumoto, K., Yoshimoto, M., Fuunaga, K., Proceedings of The 9th Asian Conference on Fluidized-Bed and Three-Phase Reactors, "Circulating Liquid Velocity, Gas Holdup and Volumetric Gas-Liquid Mass Transfer Coefficient in a Three-Phase External Loop Airlift Bubble Column" Pacific Green Bay, Wanli, Taiwan, November 21-24, 2004, 313-318.
- Reith, T., Beek, W. J., Chem. Eng. Sci. **28** (1973) 1331.
- Schumpe, A., Deckwer, W.-D., Ind. Eng. Chem. Process Des. Dev. **21** (1982) 706.
- Lamont, J. C., Scott, D. S., AIChE J. **16** (1970) 513.
- Talvy, S., Cockx, A., Line, A., AIChE J. **53** (2007) 316.
- Calderbank, P. H., Moo-Young, M. B., Chem. Eng. Sci. **16** (1961) 39.
- Akita, K., Yoshida, F., Ind. Eng. Chem. Process Des. Dev. **13** (1974) 84.